https://dx.doi.org/10.4314/ijs.v27i1.7

A HUMAN PHYSIOLOGICALLY-BASED BIO-KINETIC MODEL FOR URANIUM

Maza, D. D.
Department of Physics and Engineering Physics, Obafemi Awolowo University, Ile-Ife, Nigeria.
Corresponding Author's Email: mazadd@oauife.edu.ng
(Received: 6th January, 2025; Accepted: 24th March, 2025)

ABSTRACT

Uranium is a naturally occurring element that humans are continuously exposed to at low levels due to its pervasive presence in the environment. However, elevated exposure can pose significant health risks. Daily exposure occurs through inhaling contaminated air, ingesting uranium-contaminated food or water, and dermal contact. Once absorbed, uranium enters the bloodstream and is distributed to various organs. Traditional pharmacokinetic models, employing a compartmental approach, have been widely used to study the distribution and toxicity of absorbed uranium. This study developed a physiologically based biokinetic (PBBK) model using Python programming to simulate the absorption, distribution, metabolism, and elimination (ADME) of uranium in humans. Unlike traditional models, this approach utilizes organ-specific blood flow rates and partition coefficients for better physiological realism. The model incorporates 17 compartments, including 15 critical organs and 2 dummy compartments. Permeability rate-limited kinetics were applied to bone compartments (cortical and trabecular), while perfusion rate-limited kinetics were assumed for soft tissues such as the liver, kidneys, and gut. Simulations of fractional uranium retention in infants, children (ages 5, 10, and 15), and adults following intravenous injection show reasonable agreement with previous studies using compartmental models, particularly in predicting skeletal retention, which increases with age due to bone mineralization. For chronic oral ingestion scenarios, the model reliably reproduces observed uranium retention patterns, demonstrating its robustness across different exposure routes.

Keywords: Uranium, physiologically-based bio-kinetic, Absorption, Distribution, Elimination.

INTRODUCTION

Uranium, with atomic number, 92, is the heaviest naturally occurring element (Taylor & Taylor, 1997; Brugge & Buchner, 2011). Uranium is a ubiquitous, naturally occurring radioactive element in various environmental matrices, including soil, rocks, water, and air –(Taylor & Taylor, 1997; Dublineau *et al.*, 2006; Brugge & Buchner, 2011; Mehra & Kaur, 2020; Bangotra *et al.*, 2021). It is also present at low levels in the earth's crust. It enters the human body primarily through inhalation, ingestion, and, to a lesser extent, dermal exposure. Among these, ingestion and inhalation are the primary routes of uranium absorption (ICRP, 1991). When uranium is ingested, only a small fraction (2% to 5%) is absorbed in the gastrointestinal tract (Neuman *et al.*, 1984; Taylor & Taylor, 1997; Division of Toxicology and Human Health Sciences, 2013). The bioavailability of uranium in the digestive system is influenced by several factors, such as its chemical form, solubility, and other dietary substances that may inhibit or enhance its absorption (Taylor & Taylor, 1997; Division of Toxicology and Human Health Sciences, 2013). Inhalation of uranium occurs either as fine dust or aerosol particles. The absorption rate of inhaled uranium depends significantly on the particle size and solubility of these particles (Petitot *et al.*, 2013; Zhang *et al.*, 2022). Insoluble uranium compounds tend to remain in the lungs for extended periods, leading to prolonged exposure, whereas soluble forms of uranium compounds are more rapidly absorbed into the bloodstream (Petitot *et al.*, 2013; Zhang *et al.*, 2022). Once uranium is absorbed into the bloodstream, it is distributed to various tissues and organs, with major accumulation occurring in the kidneys, bones, liver, and other soft tissues –(Miles, 1988; Keith *et al.*, 2002; Vicente-Vicente et al., 2010).

Metabolism and Retention

Metabolic transformation of uranium does not occur in the body. Its bio-kinetics, however, depend on its solubility and chemical form. Soluble forms of uranium, such as uranium hexafluoride, are more readily absorbed and excreted, whereas insoluble forms, such as uranium dioxide, can remain in tissues longer. This increases long-term exposure risks.

Toxicity

Primarily, the health risk posed by uranium is due to its chemical toxicity, particularly its nephrotoxic effects (Limson Zamora *et al.*, 1998; Keith *et al.*, 2002; Vicente-Vicente *et al.*, 2010) . Exposure to high doses of uranium can cause acute damage to the kidneys (Limson Zamora *et al.*, 1998; Division of Toxicology and Human Health Sciences, 2013), leading to alterations in glomerular filtration rate, impairments in tubular function, and overall deterioration of renal health. In addition to its chemical toxicity, uranium presents a radiological risk, because it is an alpha emitter, albeit a relatively weak alpha emitter. The radiological danger from uranium is generally lower than its chemical toxicity, but prolonged exposure, especially from uranium retained in bones and lungs, can elevate the risk of developing cancer over time.

Pharmacokinetic Models

Pharmacokinetic models, such as physiologically based bio-kinetic (PBBK) models, are useful for understanding the absorption, distribution, metabolism, and elimination (ADME) of chemical substances in various body organs (compartments) – (Nestorov, 2007; Sager *et al.*, 2015; Yang *et al.*, 2015; Fairman *et al.*, 2020). These models typically account for factors like blood flow, organ retention characteristics, and chemical properties of the substance (Nestorov, 2007; Chetty *et al.*, 2018). Existing efforts to model uranium kinetics relied on classical compartmental approaches, dividing the body into simplified compartments like blood, kidney, liver, and skeleton, with transfer rates described by first-order kinetics "–(Neuman *et al.*, 1984; ICRP, 1991, 1994; Leggett, 1994; Wrenn *et al.*, 1994; Leggett & Pellmar, 2003; Li *et al.*, 2009). While these models provided initial insights into uranium retention and movement, they lacked physiological realism and were mostly empirical, limiting their applicability across different populations or exposure scenarios.

To provide the desired physiological realism, this study seeks to incorporate age-dependent physiological parameters, such as organ size, blood flow rates, and the use of tissue-to-blood partition coefficients to mimic the circulatory system, to predict uranium distribution across compartments, and to improve predictions for uranium retention across different life stages.

MATERIALS AND METHODS

Description of the Model

The model was developed based on fifteen (15) compartments, each representing a different organ of the human body or a group of tissues (organs) with similar blood flow properties (Figure 1). The compartments upon which this model was based are Plasma, Red blood cells (RBC), Kidney, Trabecular bone surface (TBS), Trabecular bone volume (TBV), Cortical bone surface (CBS) Cortical bone volume (CBV), Stomach; Small intestine, Gut, Liver, Vein and artery, Rest of the body (R body), and two dummy compartments (Aa and Ax). The two dummy compartments are mathematical delays inserted to model the piecemeal nature of daily inhalation and ingestion of substances, respectively. The bone compartment was split into trabecular and cortical bone compartments, which were further split into the trabecular bone surface, trabecular bone volume, cortical bone surface, and cortical bone volume, respectively. The compartments were connected by blood flow, thus mimicking the circulating blood system (Figure 1). Tissue volumes and blood flow rates were modelled as body weight and cardiac output percentages, respectively (Tables 1 and 2).

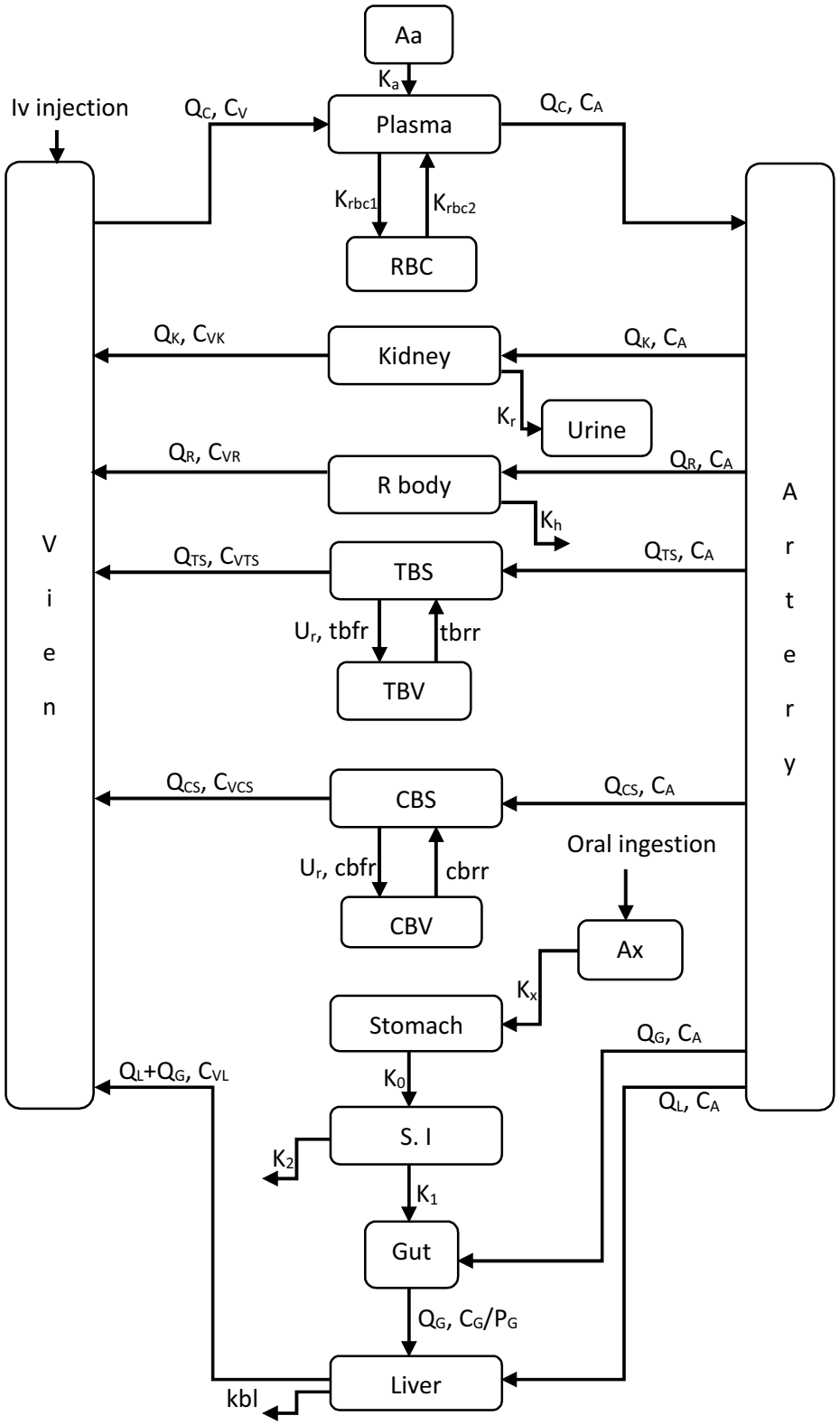

Figure 1. The model framework depicting the kinetics of uranium in the body, through the circulatory system. The cardiac output is represented by (Q_C) and blood flow rates to key organs as: kidney (Q_K), liver (Q_L), rest of the body (Q_R), gut (Q_G), trabecular bone surface (Q_{TS}), and cortical bone surface (Q_{CS}). Uranium concentrations are represented in arterial (C_A) and venous blood (C_V), with organ-specific venous concentrations denoted as C_{VK} (kidney), C_{VL} (liver), C_{VR} (rest of body), C_{VTS} (trabecular bone surface), and C_{VCS} (cortical bone surface).

Table 1: Fractional tissue volumes.

Tissue (symbol)	Fractional Volume
Bone weight (wbf)	0.122
Liver (vlf)	0.025
Kidney (vkl)	0.004
Gut (vgf)	0.017
Lung (vluf)	0.007
Blood (vblf)	0.065
Plasma (vpf)	0.041
Red blood cell	0.024
Rest body (vrf)	0.76

Table 2: Fractional blood flow rates.

Tissue (symbol)	Fractional Volume
Bone (qbf)	0.05
Liver (qlf)	0.046
Kidney (qkl)	0.175
Gut (qgf)	0.181
Rest body (qrf)	0.548

The trabecular bone was allocated 20 % of the total bone weight, while the cortical bone was allocated the remaining 80 % of the bone weight – (Jowsey, 1977; Manske et al., 2009; Ott, 2018) (Manske et al., 2009; Ott, 2018). Ninety-five percent (95 %) of the trabecular bone volume was allocated to the trabecular bone surface and 5 % to the trabecular bone matrix. On the other hand, 97 % of the cortical bone volume was allocated to the cortical bone surface, while 3 % was allocated to the cortical bone matrix (Jowsey, 1977).

Mass balance equations (differential equations) were written for each compartment to describe the flow of the chemical substance (uranium) in and out of the compartment (Table 3). Two kinetics were used to describe the movement of substances in and out of the compartments (tissues): perfusion rate-limited kinetics Figure 2a, where the distribution of the chemical substance is primarily controlled by blood flow rather than its ability to cross cell membranes

Table 3: Mass balance equations for the compartments.

Tissue	Equation
Venous Plasma	$\frac{dC_{VP}}{dt} = \frac{(Q_C * C_{VP} - (Q_C + k_{RBC2}) * C_{VP})}{V_P} + k_{RBC1} * \frac{C_{RBC}}{V_{RBC}}$
RBC	$\frac{dC_P}{dt} = \frac{k_{RBC2} * C_{VP}}{V_P} - k_{RBC1} * \frac{C_{RBC}}{V_{RBC}}$
Arterial Plasma	$\frac{dC_{AP}}{dt} = (Q_C * C_{VP} - \left(Q_K * \frac{C_K}{P_K} + Q_L * \frac{C_L}{P_L} + Q_R * \frac{C_R}{P_R} + \cdots\right))/V_A$
Kidney	$\frac{dC_K}{dt} = \frac{Q_K\left(C_{AP} - \frac{C_K}{P_K}\right)}{V_K} - k_r * C_K/V_K$
Urine	$\frac{dC_{Urine}}{dt} = k_r * C_K/V_K$
Ax	$\frac{dA_x}{dt} = Oraldose - k_x * A_x$
Stomach	$\frac{dA_{ST}}{dt} = k_x * A_x - k_0 * A_{ST}$
Small intestine	$\frac{dA_{SI}}{dt} = k_0 * A_{ST} - k_1 * A_{SI} - k_2 * A_{SI}$
Gut	$\frac{dC_G}{dt} = k_1 * A_{SI} + \frac{Q_G\left(C_{AP} - \frac{C_G}{P_G}\right)}{V_G}$
Liver	$\frac{dC_L}{dt} = \frac{\frac{Q_G * C_G}{P_G} + Q_L * C_{AP} - \frac{(Q_L + Q_G)}{P_L} - k_b * C_L}{V_L}$
Trabecular bone surface	$\frac{dC_{TBS}}{dt} = Q_{TBS} * \frac{C_{AP} - \frac{C_{TBS}}{P_{TBS}}}{V_{TBS}} + TBRR * \frac{C_{TBV}}{V_{TBV}} - UR * TBFR * \frac{C_{TBS}}{V_{TBS}}$
Trabecular bone volume	$\frac{dC_{TBS}}{dt} = UR * TBFR * \frac{C_{TBS}}{V_{TBS}} - TBRR * \frac{C_{TBV}}{V_{TBV}}$
Cortical bone surface	$\frac{dC_{CBS}}{dt} = Q_{CBS} * \frac{C_{AP} - \frac{C_{CBS}}{P_{CBS}}}{V_{CBS}} + CBRR * \frac{C_{CBV}}{V_{CBV}} - UR * CBFR * \frac{C_{CBS}}{V_{CBS}}$
Cortical bone volume	$\frac{dC_{CBS}}{dt} = UR * CBFR * \frac{C_{CBS}}{V_{CBS}} - CBRR * \frac{C_{CBV}}{V_{CBV}}$
Rest Body	$\frac{dC_R}{dt} = \frac{Q_R\left(C_{AP} - \frac{C_R}{P_R}\right)}{V_K} - k_h * C_R/V_R$
Vein	$\frac{dC_V}{dt} = (Q_K * \frac{C_K}{P_K} + Q_L * \frac{C_L}{P_L} + Q_R * \frac{C_R}{P_R} + \ldots - Q_C * C_V)/V_V$

(Kuepfer *et al.*, 2016); and permeability rate-limited kinetics, where the overall distribution or absorption of the substance is determined by the rate at which the substance crosses a biological membrane (Kuepfer *et al.*, 2016) (Figure 2b).

For compartments defined by perfusion rate-limited kinetics, the mass balance equation describing their kinetics was written as, Equation 1:

$$V_T \frac{dC_T}{dt} = Q_T(C_A - C_{VT}) \quad 1$$

Where C_T, V_T, Q_T, C_A and C_{VT} are the tissue concentration, tissue volume, blood flow rate to the tissue, concentration in arterial blood, and concentration in venous blood flowing out of the tissue, respectively, with:

$$C_{VT} = \frac{C_T}{P_T} \quad 2$$

Where P_T is the tissue partition coefficient, the ratio of the concentration of the substance in the tissue and its concentration in arterial blood.

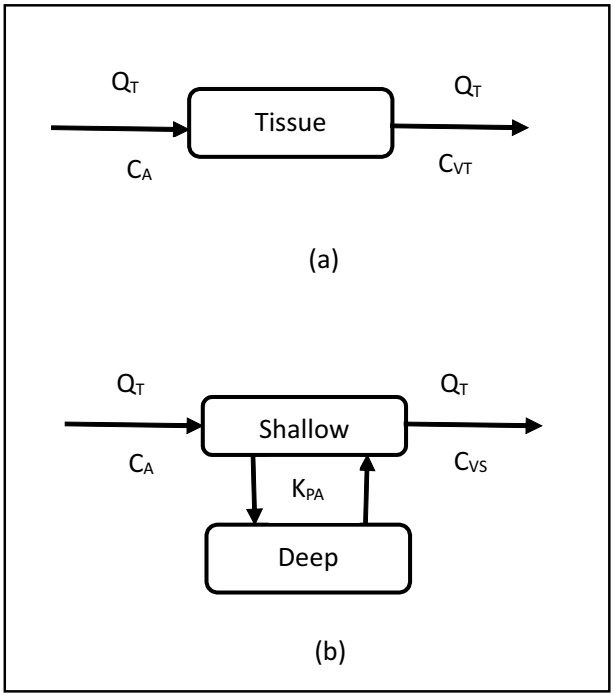

Figure 2: Movement of uranium in and out of tissues (a) perfusion rate-limited kinetics (b) permeability rate-limited kinetics. The perfusion rate is represented by the blood flow rate, while the permeability rate is represented as K_{PA}.

For tissues defined by permeation rate-limited kinetics such as the trabecular and cortical bone, the tissue was divided into two sub-compartments, the surface sub-compartment and deep sub-compartment (bone volume or bone matrix). The trabecular bone was modelled using Equations 3 and 4, while the cortical bone was modelled using Equations 5 and 6:

$$V_{TBS}\frac{dC_{TBS}}{dt} = Q_{TB}\left(C_A - \frac{C_{TBS}}{P_{TBS}}\right) - UR * TBFR * C_{TBS} + TBRR * C_{TBV} \quad 3$$

$$V_{TBV}\frac{dC_{TBV}}{dt} = UR * TBFR * C_{TBS} - TBRR * C_{TBV} \quad 4$$

$$V_{CBS}\frac{dC_{CBS}}{dt} = Q_{CB}\left(C_A - \frac{C_{CBS}}{P_{CBS}}\right) - UR * CBFR * C_{CBS} + CBRR * C_{CBV} \quad 5$$

$$V_{CBV}\frac{dC_{CBV}}{dt} = UR * CBFR * C_{CBS} - CBRR * C_{CBV} \quad 6$$

Where V_{TBS} and V_{TBV} are the trabecular bone surface and bone volume respectively, while C_{TBS} and C_{TBV} are the concentration of uranium in the trabecular bone surface and bone volume, respectively. Similarly, V_{CBS} and V_{CBV} are the cortical bone surface and bone volume respectively, while C_{CBS} and C_{CBV} are the concentration of uranium in the cortical bone surface and bone volume, respectively. $TBRR$ and $TBRR$ the trabecular bone resorption and formation rates, respective, while $CBRR$ and $CBFR$ are the cortical bone resorption and formation rates, respectively. UR is a dimensionless scaling factor for uranium. Exchange between bone surface and matrix sub-compartments is governed by the processes of bone remodelling: namely bone resorption rate (BRR) and bone formation rate (BFR). These parameters are related to the fractional bone formation rate (FBFR) as follows (OFlaherty, 1991, 1993), Equations 7 - 12:

$$BFR = FBFR * V_{bone} = BRR \quad 7$$

Where FBFR was modelled as:

$$FBFR = (0.003 + 0.321) * \exp(-0.2 * Age) + 0.081 * \exp(-0.021 * Age))/24 \quad 8$$

TBFR, TBRR, CBFR, CBRR, and were modelled as:

$$TBFR = BFR * FRAC\_T \quad 9$$

$$TBRR = BRR * FRAT\_T \quad 10$$

$$CBFR = BFR * (1 - FRAC\_T) \quad 11$$

$$CBRR = BRR * (1 - FRAC\_T) \quad 12$$

Where FRAC_T = 0.7, is the fraction of total bone formation assigned to the trabecular bone.

RESULTS AND DISCUSSION

Figures 3 to 7 illustrate the fractional retention of uranium in the kidney, liver, and skeleton across various age groups (infant, 5-year-old, 10-year-old, 15-year-old, and adult) following an intravenous injection of 1.0 µg of uranium. The simulations produced by the current model are compared with the results of Wei and co-researchers (Wei et al., 2005), demonstrating robust performance in replicating uranium bio-kinetics in these critical organs. Across all age groups, retention patterns showed a reasonable agreement within the first ten days, in the kidney and skeleton which are the primary storage sites for uranium. After the first ten days, the current model's simulation shows a faster decline in retention compared to Wei and collaborators (Wei *et al.*, 2005). The skeleton's retention increased

with age, reflecting growth-related changes in bone mineralization

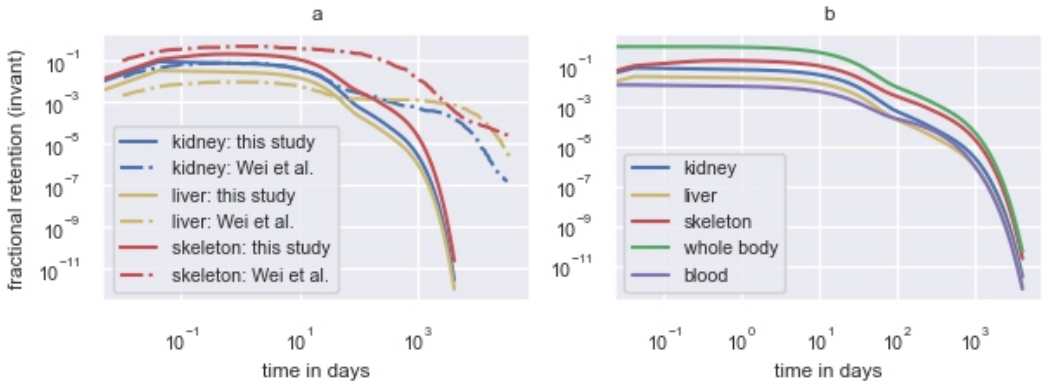

Figure 3: Fractional retention following intravenous (iv) injection of 1.0 μg for an infant (a) compares simulation of the current model in the kidney, liver, and skeleton with the simulations of Wei and collaborators (Wei *et al.*, 2005) (b) simulation of the current model for various organs.

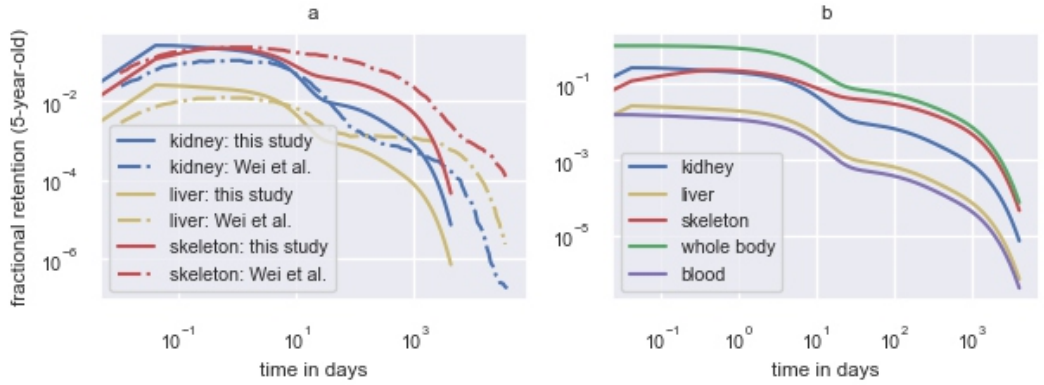

Figure 4: Fractional retention following intravenous injection of 1.0 μg for a 5-year-old (a) compares simulation of the current model in the kidney, liver, and skeleton with the simulations of Wei and collaborators (Wei *et al.*, 2005) (b) simulation of the current model for various organs.

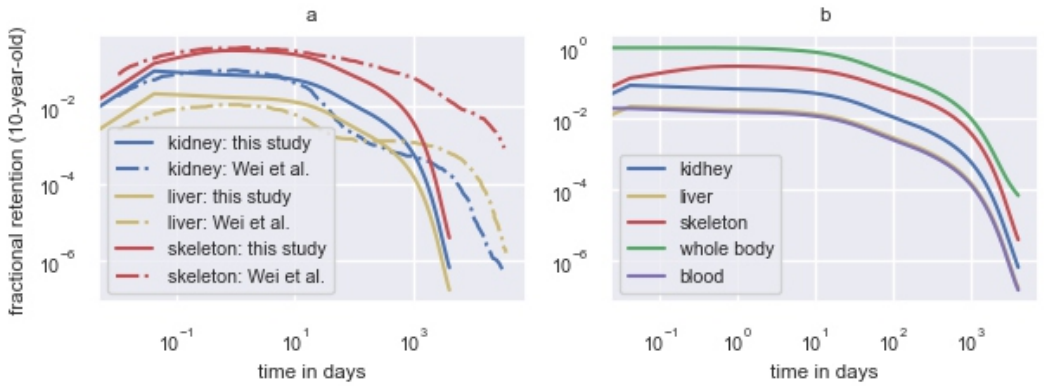

Figure 5: Fractional retention following intravenous injection of 1.0 μg for a 10-year-old (a) compares simulation of the current model in the kidney, liver, and skeleton with the simulations of Wei and collaborators (Wei *et al.*, 2005) (b) simulation of the current model for various organs.

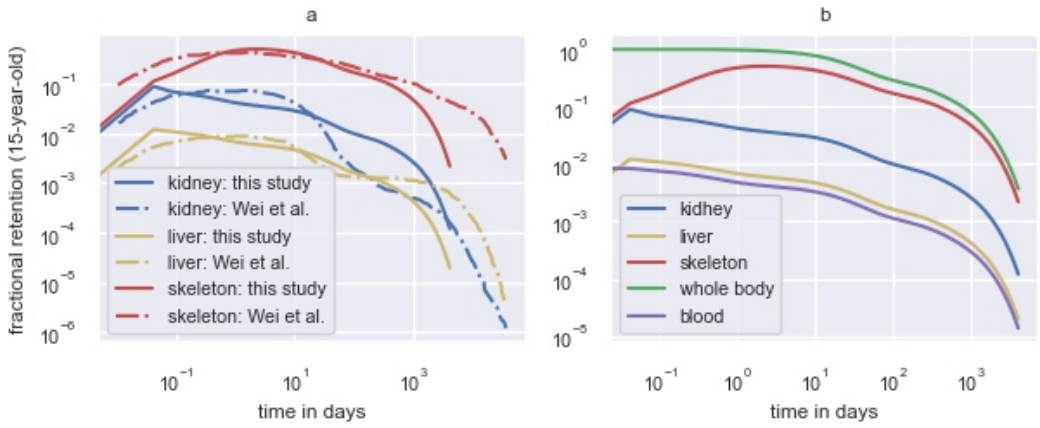

Figure 6: Fractional retention following iv injection of 1.0 μg for a 15-year-old (a) compares simulation of the current model in the kidney, liver, and skeleton with the simulations of Wei and collaborators (Wei *et al.*, 2005) (b) simulation of the current model for various organs.

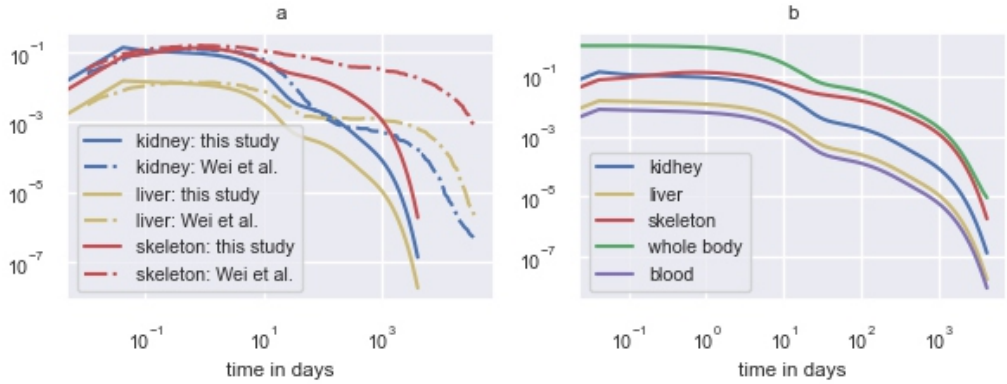

Figure 7: Fractional retention following iv injection of 1.0 μg for an adult (a) compares simulation of the current model in the kidney, liver, and skeleton with the simulations of Wei and collaborators (Wei *et al.*, 2005) (b) simulation of the current model for various organs.

Presented in Figure 8 is the fractional retention of uranium in the kidney, liver, and skeleton following chronic oral ingestion of 1.0 μg of uranium for adults. The model closely mirrors the simulation results of Wei and cohorts (Wei et al., 2005), especially in the kidney and skeleton, which are key sites of uranium deposition. The current model is capable of predicting uranium bio-kinetics across age groups and exposure scenarios, particularly in the kidney and skeleton.

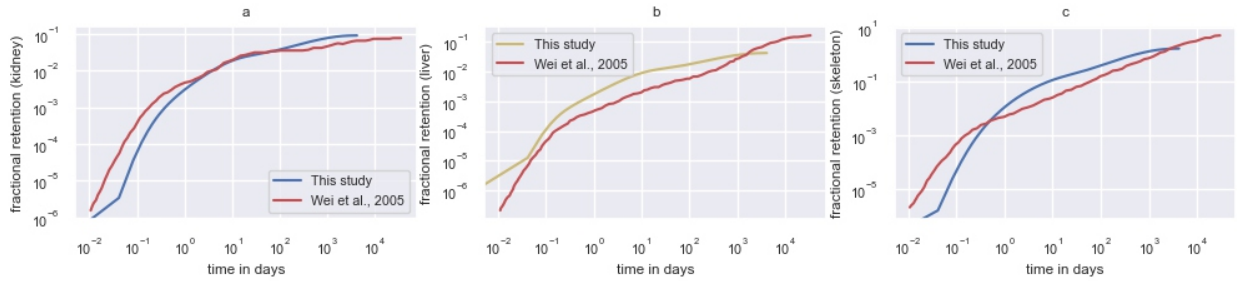

Figure 8: The simulation of fractional retention following chronic oral ingestion 1.0 μg of uranium for an adult, compared with the simulation of Wei and colleagues (Wei *et al.*, 2005) in the (a) kidney (b) liver (c) skeleton.

The results demonstrate the model's reliability in simulating uranium distribution and highlight age and exposure route as key factors in retention patterns. Future efforts could focus on refining liver-specific dynamics and expanding the model to diverse populations.

CONCLUSION

This study resulted in the development of a physiologically based bio-kinetic model capable of simulating uranium bio-kinetics across different age groups and exposure scenarios. The results demonstrated strong agreement with existing data from Wei *et al.*, particularly in predicting uranium retention in primary storage sites like the kidney and skeleton following intravenous injection. Age-dependent simulations revealed increasing skeletal retention with growth, consistent with physiological changes in bone mineralization, while the liver exhibited minor deviations likely due to differences in clearance dynamics. The model also captured the fractional retention patterns following chronic oral ingestion, further validating its reliability. Although minor discrepancies in liver retention were observed, these present opportunities for refining the hepatic component of the model. Overall, the study highlights the model's robustness in simulating uranium distribution, underscoring the importance of age and exposure routes in determining retention patterns. These findings contribute to a better understanding of uranium's behavior in human systems and provide a valuable tool for assessing its health impacts.

ACKNOWLEDGEMENT

The author acknowledges Prof. J. O. Ojo of the Department of Physics and Engineering Physics, Obafemi Awolowo University, Ile-Ife for his continuous encouragement.

FUNDING

No external funding was received for this Study.

CONFLICT OF INTEREST

The authors declare that no competing conflict of interest exists.

AUTHOR CONTRIBUTIONS

MDD: Conceptualization, Resources, Investigation, Analysis, Visualization, Original Draft, Review, and Editing.

REFERENCES

Bangotra, P., Sharma, M., Mehra, R., Jakhu, R., Singh, A., Gautam, A. S., & Gautam, S. (2021). A systematic study of uranium retention in human organs and quantification of radiological and chemical doses from uranium ingestion. *Environmental Technology & Innovation*, 21, 101360. doi: 10.1016/j.eti.2021.101360

Brugge, D., & Buchner, V. (2011). Health effects of uranium: new research findings. *Reviews on Environmental Health*, 26(4), 231-249. doi: 10.1515/REVEH.2011.032

Chetty, M., Johnson, T. N., Polak, S., Salem, F., Doki, K., & Rostami-Hodjegan, A. (2018). Physiologically based pharmacokinetic modelling to guide drug delivery in older people. *Advanced Drug Delivery Reviews*, 135, 85-96. doi: 10.1016/j.addr.2018.08.013

Division of Toxicology and Human Health Sciences. (2013). ATSDR, Public Health Statement: Uranium. Agency For Toxic Substances And Disease Registry, February. https://www.atsdr.cdc.gov/ToxProfiles/tp150-c1-b.pdf%0A

ublineau, I., Grison, S., Grandcolas, L., Baudelin, C., Tessier, C., Suhard, D., Frelon, S., Cossonnet, C., Claraz, M., Ritt, J., Paquet, P., Voisin, P., & Gourmelon, P. (2006). Absorption, accumulation and biological effects of depleted uranium in Peyer's patches of rats. *Toxicology*, 227(3), 227-239. doi: 10.1016/j.tox.2006.08.010

Fairman, K., Li, M., Kabadi, S. V., & Lumen, A. (2020). Physiologically based pharmacokinetic modeling: A promising tool for translational research and regulatory toxicology. *Current Opinion in Toxicology*, 23-24(March), 17-22. doi: 10.1016/j.cotox.2020.03.001

ICRP. (1991). Annual limits on intake of radionuclides by workers based on the 1990 recommendations. A report from Committee 2 of the International Commission on Radiological Protection. In *Annals of the ICRP* (Vol. 21, Issue 4).

ICRP, I. C. for R. P. (1994). *Annals of the ICRP, Publication 69: Age-dependent Doses to Members of the Public from Intake of Radionuclides: Part 3 Ingestion Dose Coefficients*.

Jowsey, J. (1977). Cortical and Trabecular Bone. In: *The Bone Biopsy. Topics in Bone and Mineral Disorders*. Springer US.
doi: 10.1007/978-1-4684-2379-2

Keith, S., Obaid, F., Nickolette, R., Franco, S., Sharon, W., Lisa, I., Fernando, L., Daniel, P., David, W., & Gary, D. (2002). Toxicological Profile for Uranium. In *ATSDR's Toxicological Profiles* (Issue February). CRC Press.
doi: 10.1201/9781420061888_ch157

Kuepfer, L., Niederalt, C., Wendl, T., Schlender, J. F., Willmann, S., Lippert, J., Block, M., Eissing, T., & Teutonico, D. (2016). Applied Concepts in PBPK Modeling: How to Build a PBPK/PD Model. *CPT: Pharmacometrics and Systems Pharmacology,* 5(10), 516-531.
doi: 10.1002/psp4.12134

Leggett, R. W. (1994). Basis for the icrp's age-specific biokinetic model for uranium. *Health Physics,* 67(6), 589-610.
doi: 10.1097/00004032-199412000-00002

Leggett, R. W., & Pellmar, T. C. (2003). The biokinetics of uranium migrating from embedded DU fragments. *Journal of Environmental Radioactivity,* 64(2-3), 205-225.
doi: 10.1016/S0265-931X(02)00050-4

Li, W. B., Karpas, Z., Salonen, L., Kurttio, P., Muikku, M., Wahl, W., Höllriegl, V., Hoeschen, C., & Oeh, U. (2009). A compartmental model of uranium in human hair for protracted ingestion of natural uranium in drinking water. *Health Physics*, 96(6), 636-645.
doi: 10.1097/01.HP.0000345023.46165.1c

Limson Zamora, M., Tracy, B. L., Zielinski, J. M., Meyerhof, D. P., & Moss, M. A. (1998). Chronic ingestion of uranium in drinking water: A study of kidney bioeffects in humans. *Toxicological Sciences*, 43(1), 68-77.
doi: 10.1006/toxs.1998.2426

Manske, S. L., Liu-Ambrose, T., Cooper, D. M. L., Kontulainen, S., Guy, P., Forster, B. B., & McKay, H. A. (2009). Cortical and trabecular bone in the femoral neck both contribute to proximal femur failure load prediction. *Osteoporosis International,* 20(3), 445-453.
doi: 10.1007/s00198-008-0675-2

Mehra, R., & Kaur, S. (2020). Uranium in Plants and the Environment (D. K. Gupta & C. Walther (eds.)). Springer International Publishing.
doi: 10.1007/978-3-030-14961-1

Miles, J. (1988). Health risks of radon and other internally deposited alpha-emitters. *Endeavour*, 12(4), 197.
doi: 10.1016/0160-9327(88)90189-5

Nestorov, I. (2007). Whole-body physiologically based pharmacokinetic models. *Expert Opinion on Drug Metabolism and Toxicology,* 3(2), 235-249.
doi: 10.1517/17425255.3.2.235

Neuman, W. F., Fleming, R. W., Dounce, A. L., Carlson, A. B., O'leary, J., & Mulryan, B. (1984). *THE DISTRIBUTION INJECTED AND EXCRETION URANIUM*.

O'Flaherty, J. E. (1991). Physiologically Based Models for Bone-Seeking Elements II. Kinetics of Lead Deposition in Rats. *Toxicology and Applied Pharmacology,* 111, 313-331.

O'Flaherty, J. E. (1993). Physiologically Based models for Bone-seeking Elements IV. Kinetics of Lead Deposition in Humans. *Toxicology and Applied Pharmacology,* 118, 16-29.

Ott, S. M. (2018). Cortical or Trabecular Bone: What's the Difference? *American Journal of Nephrology*, 47(6), 373-375.
doi: 10.1159/000489672

Petitot, F., Lestaevel, P., Tourlonias, E., Mazzucco, C., Jacquinot, S., Dhieux, B., Delissen, O., Tournier, B. B., Gensdarmes, F., Beaunier, P., & Dublineau, I. (2013). Inhalation of uranium nanoparticles: Respiratory tract deposition and translocation to secondary target organs in rats. *Toxicology Letters,* 217(3), 217-225. doi: 10.1016/j.toxlet.2012.12.022

Sager, J. E., Yu, J., Ragueneau-Majlessi, I., & Isoherranen, N. (2015). Physiologically based pharmacokinetic (PBPK) modeling and simulation approaches: A systematic review of published models, applications, and model verification. *Drug Metabolism and Disposition,* 43(11), 1823-1837. doi: 10.1124/dmd.115.065920

Taylor, D. M., & Taylor, S. K. (1997). *Environmental Uranium and Human Health.* 12(3), 147-158. doi: 10.1515/reveh.1997.12.3.147

Vicente-Vicente, L., Quiros, Y., Pérez-Barriocanal, F., López-Novoa, J. M., López-Hernández, F. J., & Morales, A. I. (2010). Nephrotoxicity of uranium: Pathophysiological, diagnostic and therapeutic perspectives. *Toxicological Sciences,* 118(2), 324-347. doi: 10.1093/toxsci/kfq178

Wei, B. L., Roth, P., Wahl, W., Oeh, U., Höllriegl, V., & Paretzke, H. G. (2005). Biokinetic modeling of uranium in man after injection and ingestion. *Radiation and Environmental Biophysics,* 44(1), 29-40. doi: 10.1007/s00411-005-0272-0

Wrenn, M. E., Bertelli, L., Durbin, P. W., Singh, P. N., Lipsztein, J. L., & Eckerman, K. F. (1994). A Comprehensive Metabolic Model for Uranium Metabolism and Dosimetry Based on Human and Animal Data. *Radiation Protection Dosimetry*, 53(1-4), 255-258.

Yang, X., Doerge, D. R., Teeguarden, J. G., & Fisher, J. W. (2015). Development of a physiologically based pharmacokinetic model for assessment of human exposure to bisphenol A. *Toxicology and Applied Pharmacology*, 289(3), 442-456. doi: 10.1016/j.taap.2015.10.016

Zamora, M. L., Tracy, B. L., Zielinski, J. M., Meyerhof, D. P., Moodie, G. B., & Falcomer, R. (n.d.). Uranium Gastrointestinal Absorption in Humans: A Chronic Exposure Study.

Zhang, L., Chu, J., Xia, B., Xiong, Z., Zhang, S., & Tang, W. (2022). Health Effects of Particulate Uranium Exposure. *Toxics*, 10(10), 1-19. doi: 10.3390/toxics10100575